Fermi surface of UGe_2 in the paramagnetic phase

M. Biasini*
ENEA, Via Don Fiammelli 2, 40129 Bologna, Italy

R. Troc
Trzebiatowski Institute of Low Temperature and Structure Research, P.O. Box 1410, Wroclaw, Poland
(Received 27 June 2003; revised manuscript received 27 August 2003; published 29 December 2003)

We measured the two-dimensional angular correlation of the positron annihilation radiation on a single crystal of UGe_2 in the paramagnetic phase. The results of the Lock-Crisp-West transformation, yielding a projection of the electron-positron $\boldsymbol{k}$ density, are compared to band-structure calculations in local-density approximation treating the U $5f$ electrons as *itinerant*, *fully localized* or according to the assumption that *two of the three 5f electrons are localized*. The *fully localized* model shows the best agreement with the experiments.

DOI: 10.1103/PhysRevB.68.245118 PACS number(s): 71.27.+a, 71.18.+y, 78.70.Bj, 71.60.+z

I. INTRODUCTION

The recently observed coexistence of magnetic ordering, superconductivity, and heavy fermion behavior in some rare-earth and actinide intermetallic compounds has emerged as a central topic of solid-state physics.[1,2] In the past, these three phenomena were always considered antagonist. For example, it was assumed that in a heavy fermion the Kondo effect would lead to the vanishing of the magnetic moment as the result of the fluctuations (spin flips) caused by the interactions between the *f*-like electron localized at the rare earth site and the conduction electrons.[1] Concerning magnetism and superconductivity, the effect of applying a magnetic field to a standard Bardeen-Cooper-Schrieffer (BCS) superconductor, with destruction of superconductivity, is a well-known result. Surprisingly, one can find a large class of heavy (or moderately heavy) fermions where the strongly correlated state coexists with the magnetic ordering. A notable example is the archetype dense Kondo lattice system CeB_6; other compounds are $CeAl_3$, $CePd_2Si_2$, $CeRh_2Si_2$, UGe_2, URhGe, $U(Ni,Pd)_2Al_3$, $ZrZn_2$, and $CeIn_3$.[3] Of these systems, several have also displayed the fascinating interaction between superconductivity and (anti)ferromagnetism. Indeed, the fact that superconductivity is observed in a narrow interval of pressure, just about the point of disappearance of magnetic order, and not at higher pressures, suggests that these two phenomena are intimately related.[2] Among the compounds mentioned above, UGe_2, URhGe, and $ZrZn_2$ are probably the most interesting, owing to their ferromagnetic order which may sound more antinomic to standard BCS superconductivity. In these systems, the superconducting phase is found within the ferromagnetic phase and disappears in the paramagnetic region. In light of these findings, it has been argued that a spin triplet magnetically mediated interaction should cause superconductivity.[2] A natural consequence of this conjecture is that the electrons carrying the magnetic moments should be itinerant at the onset of superconductivity. This paper aims at clarifying this issue in the archetype ferromagnetic superconductor UGe_2. Its Sommerfeld coefficient γ and Curie temperature T_C (at atmospheric pressure) are 30 mJ/(K^2 mol) and 52 K, respectively. By raising pressure, γ increases steeply near 11kbar, to reach $\simeq$110 mJ/(K^2 mol). The Fermi surface (FS) has been studied extensively in the ferromagnetic phase and under application of pressure via the de Haas–van Alphen (dHvA) technique.[4–6] In agreement with magnetization, resistivity, and magnetoresistance measurements at ambient and high pressure,[7,8] the dHvA experiments separate two magnetically ordered phases in the temperature-pressure diagram, denoted by the authors of Ref. 5 as strongly polarized phase (SPP), for $p<p_c^*(T)$, and weakly polarized phase (WPP), for $p_c^*(T)<p<p_c(T)$.[5] The dHvA measurements in the SPP were interpreted according to band-structure calculations which treat the $5f$ electrons as itinerant.[4] Indeed, it was suggested that the distinct decrease in the value of the moment between the paramagnetic state ($\mu_{eff}\simeq 2.7\mu_B$) and the ferromagnetic state ($\mu_s\simeq 1.4\mu_B$) is consistent with band magnetism.[6] However, it is worth recalling that (i) the low ratio μ_{eff}/μ_s in UGe_2 is typical in uranium compounds,[9,10] regardless of the itinerancy or localization of the $5f$ electrons; (ii) to our knowledge, crystal-field effects, which usually decrease the value of the saturation moment have not been taken into account, as yet.

Furthermore, in the WPP and paramagnetic phase [i.e., for $p>p_c^*(T)$] the agreement between *f*-band calculation and dHvA experiment is lost.[4] In this regard, it is worth mentioning the LDA+U band-structure calculation of Shick and Pickett[11] where U is varied empirically until an agreement between total magnetic moment (orbital plus spin) and experimental one is found. The calculated FS (in the ferromagnetic phase) shows a *nesting feature*, i.e., a quasi-two-dimensional shape along planes perpendicular to the easy axis of the magnetization (spanning vector $\boldsymbol{Q}\approx(0.45\times 2\pi/a,0,0)$, where a is the lattice constant along the [1,0,0] direction). Shick and Pickett[11] and other authors[2,12] suggest that the nesting should promote strong magnetic interactions between carriers with parallel spin located periodically in space at distance $L=2\pi/|\boldsymbol{Q}|$, in support of a magnetically mediated *p*-wave triplet pairing. This hypothesis is consistent with magnetoresistance experiments which suggest the existence of open orbits perpendicular to the *b* axis.[13]

The purpose to investigate the FS of UGe_2 via the two-dimensional angular correlation of the positron annihilation radiation (2D-ACAR) experiment in the paramagnetic phase (at ambient pressure) is twofold: (i) since the measurements are performed with a weak magnetic field ($B<2$ T) we can avoid the perturbation due to the strong B fields applied in the dHvA experiments, which may hinder the detection of the unperturbed FS owing to Zeeman effect and possible magnetic breakdown; (ii) as it will be shown, an essential difference in one cylindrical FS manifold, calculated via the standard local-density approximation (LDA) method or other models, concerns the electronlike or holelike character of this FS sheet. Whereas dHvA is unable to detect these differences, a 2D-ACAR experiment, by probing all the electronic states, can provide a clear cut evidence in favor of one or another model.

In detail, by measuring the distribution $N(\theta_x,\theta_y)$ of the deviation angles from anticollinearity of the annihilation γ rays, the experiment determines a two-dimensional (2D) projection $[\rho_{2D}^{ep}(p_x,p_y)]$ of the 3D electron-positron (ep) momentum density, $\rho^{ep}(\boldsymbol{p})$.[14] The contribution to $\rho^{ep}(\boldsymbol{p})$ from the conduction bands l is discontinuous at points $\boldsymbol{p}_{F_l}=(\boldsymbol{k}_{F_l}+\boldsymbol{G})$, where $\boldsymbol{G}$ is a reciprocal-lattice vector and $\boldsymbol{k}_{F_l}$ are the reduced Fermi wave vectors in the first Brillouin zone (BZ). The standard Lock-Crisp-West (LCW) transformation,[15] extensively used in the data analysis of the 2D ACAR spectra, reinforces these discontinuities by folding the momentum distribution $\rho^{ep}(\boldsymbol{p})$ back onto the first BZ by translation over the appropriate vectors $\boldsymbol{G}$. If the summation is performed over a sufficient portion of momentum space the result is[16]

$$\rho_{LCW}^{ep}(\boldsymbol{k})=\sum_n \theta(E_F-\epsilon_{\boldsymbol{k},n})\int |\psi_{\boldsymbol{k}}^n(\boldsymbol{r})|^2|\phi(\boldsymbol{r})|^2 g_{\boldsymbol{k}}^n(\boldsymbol{r})d\boldsymbol{r}. \tag{1}$$

Here ϕ denotes the positron wave function, $\epsilon_{\boldsymbol{k},n}$ is the energy eigenvalue of the electron from band n with Bloch wave vector $\boldsymbol{k}$ and wave function $\psi_{\boldsymbol{k}}^n$. The factor $g_{\boldsymbol{k}}^n(\boldsymbol{r})$ accounts for the ep correlations.[17] In general, although the mapping of the FS is facilitated when the overlap integral in Eq. (1) is a weakly varying function of $\boldsymbol{k}$, the FS discontinuities [marked by the step function of Eq. (1)] are not shifted by this $\boldsymbol{k}$ dependence. If, as in the present case, the LCW transformation is applied to a projection of $\rho^{ep}(\boldsymbol{p})$, the result of Eq. (1) yields a projection of the electron-positron $\boldsymbol{k}$-space density in the BZ and, consequently, information on the Fermi volume. In this work, we present the results of 2D-ACAR measurements over few single crystals of UGe_2 for various crystallographic orientations. The measurements are complemented by *ab initio* band-structure calculations obtained via the full potential linearized augmented plane-wave (FLAPW) method[18] within the LDA. The calculations treat the $5f$ electrons with different starting assumptions. We discuss our results in the light of previous dHvA experiments and calculations.

II. EXPERIMENTAL PROCEDURES AND DETAILS OF THE CALCULATIONS

The crystal structure of UGe_2 is orthorhombic (space group $Cmmm$), with lattice constant $a=4.018$ Å, $b=15.083$ Å, $c=4.098$ Å.[8] The 2D-ACAR experiments were performed on single crystals grown according to the procedure described in Ref. 8. Three single crystals (s1, s2, s3) were utilized for the measurements. Crystals s1 and s2 were (001) plates, (of sizes $5\times5\times0.5$ mm^3 for the [100], [010], and [001] directions, respectively) whereas s3 was a (100) plate (of sizes $0.5\times5\times5$ mm^3). Due to the geometry of our spectrometer, in the latter case the easy axis of the magnetization ($a=[100]$) was parallel to the direction of the 1.8 T focusing magnetic field. The sizes of the crystals were larger than the image of the ^{22}Na positron source onto the sample ($\simeq4$ mm^2). Moreover, a 12-cm-thick tungsten collimator shielded the detectors from any radiation not emitted directly from the samples.

The measurements were carried out with a setup based on a pair of Anger cameras, described in detail in Ref. 19. The very long b axis (with the consequent reduction of the BZ along [010]) suggested to acquire the angular correlation spectra with integration direction parallel to [010]. The spectra were acquired at the temperature of 60 K in a vacuum of 1×10^{-6} torr. Moreover, the sample s2 was measured also at room temperature, to investigate any instability due to the vicinity of the low-temperature acquisition to the Curie temperature ($T_C=52$ K). Each spectrum accumulated $\approx3\times10^8$ raw coincidence counts in a (292×292) matrix with a bin size of (0.02×0.02) a.u.^{2}. The estimated overall experimental resolution, obtained by combining the intrinsic angular resolution with the intrinsic sizes of the positron-source spot at the sample and the thermal motion of the positron (~0.03 a.u., at 60 K), was (0.08,0.13) a.u. at 60 K for the p_z and p_y directions, equivalent to 10% and 17% of the projected BZ, respectively. The spectra were subjected to the usual correction procedures and deconvoluted according to the Van Citter–Gerhardt algorithm.[20] In the 2D-ACAR studies it is common practice to perform a preliminary analysis of the anisotropy $A(p_x,p_y)$ of the angular correlation spectra. This is defined as

$$A(p_x,p_y)=\rho_{2D}^{ep}(p_x,p_y)-\rho_{2D}^{ep}(\sqrt{p_x^2+p_y^2}), \tag{2}$$

where $\rho_{2D}^{ep}(p_x,p_y)$ is the experimental spectrum and $\rho_{2D}^{ep}(\sqrt{p_x^2+p_y^2})$ represents its angular average.[21] Beyond checking the integrity and proper symmetry of the data, $A(p_x,p_y)$ gives information on the FS topology whenever the anisotropy of the projected electron-positron momentum density, $\rho_{2D}^{ep}(p_x,p_y)$, is mostly caused by the discontinuities of the electron momentum density of the conduction band at the $\boldsymbol{k}_F+\boldsymbol{G}$ points. These discontinuities occur along directions which have the BZ, rather than the radial symmetry.

Figure 1 shows the anisotropy part of the (010) projection of UGe_2. The amplitude variation corresponds to $\simeq7\%$ of the maximum, equivalent to ~18 times the statistical uncertainty of the maximum. It is worth noticing the almost fourfold symmetry, due to the similarity of the lattice constants a

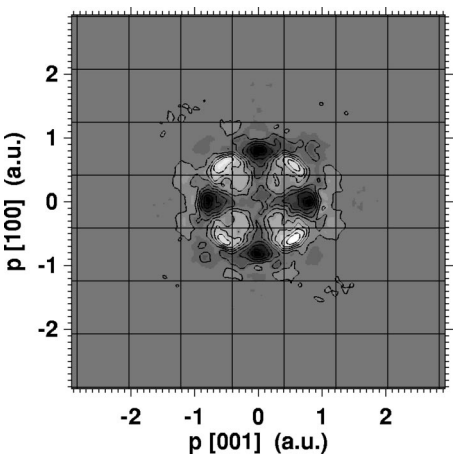

FIG. 1. Anisotropy of the measured electron-positron momentum distribution $\rho^{ep}(\boldsymbol{p})$ of UGe_2 for integration along the [010] direction. The spectrum was smoothed with an equally weighted smoothing array of (0.1×0.1)a.u.^{2} The borders of the projected first BZ in a repeated zone scheme are shown. In this and all following grey scale figures white corresponds to high intensity and black to low intensity. 1 momentum a.u.$=7.3\times10^{-3}m_0c$, where m_0 is the electron rest mass and c is the speed of light.

and c. Nevertheless, at higher momenta the departure from a C_{4v} symmetry appears quite clearly [see, for example, the conjugate pairs (1.2, 0.4) a.u. and (0.4, 1.2) a.u.].

The reproducibility of the results was tested by comparing the spectra obtained from the aforementioned three single crystals, s1, s2, s3, having plate axes parallel to [001] (s1,s2) and [100] (s3), respectively. Since in all cases the integration direction was $b=[010]$ the anisotropies of s1 and s2 were identical, and rotated 90° with respect to the anisotropy of s3, according to the expectations.

Since the temperature of our measurements ($T\sim60$ K) was rather close to T_C ($T_C=52$ K), the two 2D-LCW spectra of sample s2, collected at room temperature and at 60 K, were inspected for possible differences. The analysis showed that, apart from the modest degradation in the experimental resolution due to the positron motion ($\sim20\%$), no temperature effect attributable to low-temperature magnetic fluctuations was observed.

After the analysis in momentum space, the LCW transformation[15] was applied. For the s2 sample, the total amplitude variation of the unsymmetrized experimental LCW density was 5.4%, equivalent to ~26 times the statistical error of the maximum. The results from samples s1 and s3, fully compatible with what established for s2, are not shown. Further details of the data analysis can be found in Ref. 20.

The band-structure calculation[18] adopted three ways to treat the $5f$ electrons of uranium.

(1) The $5f$ electrons were considered as ordinary band electrons (f band).

(2) The $5f$ electrons were regarded as core states (f core). Whereas the f band method complied fully with the recipe of the LDA, the f core calculation was accomplished by forcing a U $5f^3$ core configuration. The energy parameter for the LAPW linearization of the $5f$ orbitals was set at very high value (~2 Ry) thus excluding the U f component from the valence states.

TABLE I. Fermi volumes expressed in percent of the BZ [FV (BZ %)] of the three conduction bands obtained from the f-core and f-band calculation. The increasing number of the bands refers to the increasing energy of the eigenstates.

Model	Band no.	Electron/hole	FV (BZ %)
f band	43	Electron	30.0
f band	42	Hole	28.5
f band	41	Hole	1.5
f core	40	Electron	33.0
f core	39	Hole	33.0
f core	38	Hole	0.4

(3) We treated only two $5f$ electrons as core electrons (dual $5f$), allowing band $5f$ states to be occupied, i.e., releasing the constraint of the energy parameter for the $5f$ orbital adopted in the open f core treatment. By allowing a dual behavior of the $5f$ electrons it was possible to interpret successfully the dHvA experiments in UPt_3 (Ref. 22) and to describe the 2D-ACAR results in UGa_3.[23] The coexistence between itinerant and localized $5f$ states in UGe_2 was proposed by Yaouanc *et al.* who measured the relaxation of the positive muon spin across T_C.[24] A similar conclusion has been drawn from magnetoresistance results, which revealed strong magnetic fluctuations at $T^*=T_C/2$ K.[8] This instability suggested the onset of magnetic states of itinerant character, coexisting with the $5f$ localized states.

For each calculation, the plane-wave expansion in the interstitial region was truncated at the maximum wave vector $K_{max}=3$ a.u. Inside the muffin-tin (MT) spheres (having MT radii $R=2.6$ a.u. and $R=2.5$ a.u. for U and Ge, respectively) we used spherical harmonics with angular momenta up to $l_{max}=10$ for the potential, the charge density, and the wave functions. The irreducible part of the BZ was sampled using 150 special k points according to the linear tetrahedra method. The self-consistent calculation was performed including spin-orbit coupling at each variational step. Having obtained the band structure and the Fermi level (E_F), we calculated the so-called electronic occupancy which consists of the number of occupied bands in a rectangular mesh of the BZ (an equivalent of 5800 mesh points for the nonprimitive prism of sizes $[0:2\pi/a]\times[0:2\pi/b]\times[0:2\pi/c]$ were utilized). This quantity was integrated along the projection direction and compared to $\rho^{ep}_{LCW}(\boldsymbol{k})$ defined in Eq. (1), within the approximation of a $\boldsymbol{k}$-independent overlap integral.

Since the lattice structure of UGe_2 contains two formula units, the calculation yields compensated metals for either the f-band or f-core models. In both cases three bands cross the Fermi level. As shown in Table I, the Fermi volumes fulfill the compensation requirements.

III. RESULTS AND DISCUSSION

The itinerancy or localization of the f electrons in heavy fermion systems has intensively been investigated for almost

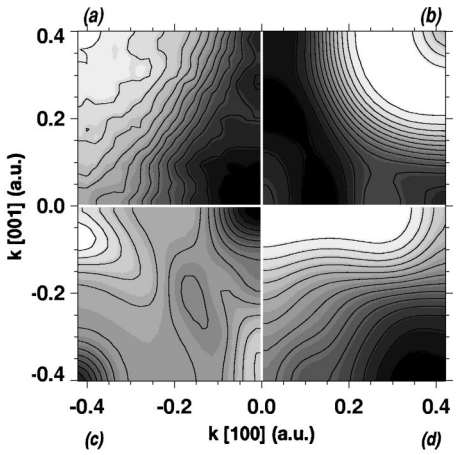

FIG. 2. Quadrant (a) 2D $\rho^{ep}_{LCW}(k_x,k_y)$ density of UGe_2 obtained from LCW folding the 2D experimental projection $\rho^{ep}(p_x,p_y)$, with p_z along the [010] axis). The contour level spacing corresponds to 0.4% of the maximum. Quadrants (b), (c), and (d): projected FLAPW theoretical occupancies (see text): (b) *f*-core model, (c) dual model (two $5f$ electrons in core), (d) *f*-band model. The matrix sizes are equivalent to $2\pi/a\times 2\pi/c$. 1 Bloch wave vector a.u.= 1 momentum a.u./$\hbar = 1/a_0 = 1.89$ Å^{-1}, where a_0 is the Bohr radius.

two decades.[3,25] As mentioned above, there are many exceptions to the so-called ''standard heavy fermion behavior'' which, in a nutshell, claims localization of the *f* electrons at high temperature and hybridization with s,p,d states below some characteristic temperature[26] to account for the high values of the γ coefficients and the vanishing of the magnetic moment. Concerning UGe_2, on the one hand, susceptibility measurements above T_C yield an effective paramagnetic moment $\mu_{eff}\approx 2.7\mu_B$/U, which is lower than the free ion value of $3.6\mu_B$ for the f^3 configuration, suggesting hybridization of $5f$ electrons with conduction states (in the paramagnetic phase).[2] On the other hand, the straight-line shape of the inverse susceptibility vs *T* curve (Curie-Weiss-like) is typical of local unhybridized moments.[2] As discussed above, the reduction of the moment is not necessarily linked only to hybridization phenomena.

With this caveat, we compare the electronic occupancies of the *f*-core and the *f*-band models to the experimental results. To this end, Fig. 2 shows two-dimensional line integrals along the [010] direction of the *f*-core and *f*-band occupancies [quarters 2(b) and 2(d), respectively] compared to the 2D-LCW folded data of the 2D-ACAR measurement for the same projection direction [quarter 2(a)]. The theoretical results of Fig. 2 were convoluted with an experimental resolution [(0.1,0.1) a.u.] since no deconvolution procedure applied to the experimental data can restore perfectly the ''true'' data. The *f*-core model shows a fairly good agrement with the experiment in the shape of the highs centered at the corners of the BZ and (to a lesser extent) in the central part of the projected BZ. It is worth noticing that the former structure appears also in the anisotropy of the experimental $\rho^{ep}_{2D}(\boldsymbol{p})$ (Fig. 1) at the corners of the first projected BZ. Conversely, the main features of the *f*-band calculation are practically opposite to the experimental ones. These features are independent of small shifts of E_F (5 mR) upward or downward. Indeed, since in an *f*-band calculation the conduction bands, having often high *f*-electron character, are usually quite flat, small changes in E_F could yield dramatic changes in the Fermi surface. However, in this case, the discrepancy with the experiment is not lifted by these moderate shifts (which, inevitably, lead to an incorrect Fermi volume). We also note that, whereas the discrepancy between *f*-band model and experiment is too large to be caused simply by an electron-positron $\boldsymbol{k}$-dependent overlap integral [as described by Eq. (1)] one cannot attribute the discrepancy between *f*-core model and experiment either to a positron effect or to the consequence of an oversimplified band-structure calculation.

To investigate the latter possibility, we compared the experiment to the dual-$5f$ calculation, described above and shown in quarter 2(c). The dual-$5f$ occupancy differs drastically from that of the *f*-band model but disagrees with the experiment more than the *f*-core calculation. We have tentatively tried to reduce further the hybridization of the valence states with the $5f$ orbitals by increasing the occupancy of the $5f$ core state to the noninteger number of 2.5 electrons/U.[27] However, although the partial *f* charge of the valence states in the U spheres decreased noticeably (from 0.78 to 0.48 electrons) there was no improvement in the comparison with the experiment. Altering slightly the position of E_F did not lead to clear improvement in the comparison with the experiment.

It is worth pointing out that the highs (lows) at the corners of the projected BZ produced by the *f*-core (*f*-band) model are mostly caused by the electronlike columnar structures from band 40 (holelike columnar structures from band 42). Figure 3 shows the calculated cylindrical FS's at issue.

Although the *f*-band columns [see Fig. 3b)] are somewhat more irregular, the extremal cross-sectional areas lead to dHvA frequencies (υ_{dHvA}) which do not differ substantially from those yielded by the *f*-core model. We get (for *B* parallel to [010]) $\upsilon_{dHvA}\approx 8\times 10^7$ G within 10% for both models. Therefore, we claim that in this system the dHvA experiment is not appropriate to address the question over localization or itinerancy of the $5f$ electrons, which is revealed mostly by the electronlike or holelike characters of the FS's shown in Fig. 3. Indeed, the general features of the electronlike *f*-core occupancy are reflected clearly in the 2D-ACAR data. We also note that the columnar structures of the *f*-core model show much more distinct nesting features than the *f*-band ones. However, unlike Shick and Pickett who propose (in the ferromagnetic phase) nesting along the easy axis of the magnetization ($a=[100]$),[11] the spanning vector $\boldsymbol{Q}$ detected here is parallel to [001] ($\boldsymbol{Q}=[0,0,0.55(2\pi/c)]$). Figure 4(a) shows in greater detail the nesting feature discussed. This structure persists for over $\simeq 50\%$ of $2\pi/b$. Figure 4(b) shows a corresponding slice of the holelike FS from band 42 which turns out to be in good agreement with Fig. 7 of Ref. 4, caption *band 20-hole*. As discussed above, since the unoccupied states lie inside the dHvA orbits (dark region), this FS sheet is inconsistent with the 2D-ACAR experiment. Although our results were obtained in the paramagnetic phase,

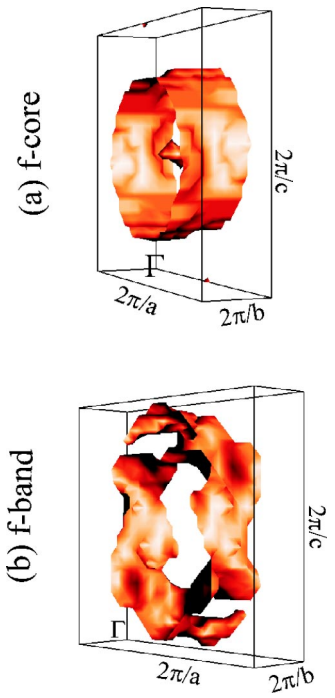

FIG. 3. (Color online) (a) The electronlike cylindrical FS of UGe_2 from band 40 produced by the *f*-core model, discussed in the text. To facilitate its visualization, the FS is shown in the nonprimitive prism of sizes $[0{:}2\pi/a]\times[0{:}2\pi/b]\times[0{:}2\pi/c]$. (b) Same as (a) for the holelike cylindrical FS from band 42 produced by the *f*-band model.

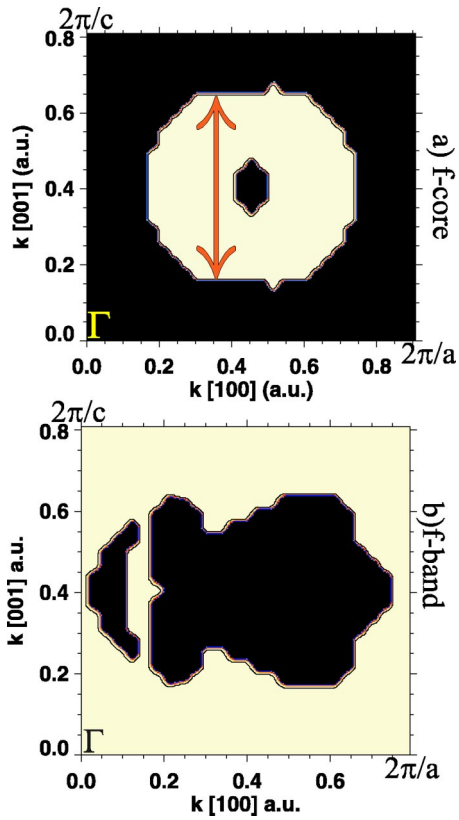

FIG. 4. (Color online) (a) Section of the electronlike cylindrical FS of UGe_2 from band 40 produced by the *f*-core model, discussed in the text. The arrow connects the parallel profiles of the FS. (b) Same as (a) for the holelike cylindrical FS from band 42 produced by the *f*-band model.

this evidence may hint that the *f* electrons should not contribute directly to superconductivity. Indeed, some preliminary experiments below T_C indicate that the momentum density is unaffected by the ferromagnetic transition. While these results are waiting for further confirmation, we recall that they are consistent with previous 2D-ACAR experiments on transition metals. For example, in the case of Ni no noticeable changes in the FS across the ferromagnetic transition and in the span of several hundred kelnin was reported.[28] If the carriers of the magnetic moment were not involved directly in the pairing causing superconductivity one should wonder which electrons are left to form the Cooper pairs in this class of materials. Recently, we have proposed for the antiferromagnetic superconductor[29] $CeIn_3$ that the indirect exchange interaction between the *localized f* electrons, which is transmitted via the polarization of the conduction electrons, could provide the pairing mechanism in an analogous manner to that provided by the phonon–conduction-electron interaction in standard BCS superconductors. The nesting feature shown in Fig. 4(a), which does not involve *f* electrons, supports a similar mechanism.[20] We recall that in UGe_2 the nearest U atoms are at a distance greater than 3.9 Å, which is significantly larger than the Hill limit[30] beyond which the direct *f*-*f* overlap ceases. Therefore, it is conceivable that, in the absence of substantial hybridization of the $5f$ orbitals with s,p,d states, the above-mentioned mechanism takes place (in this case with a positive exchange integral, to account for ferromagnetic pairing).

In conclusion, we have shown clear cut evidence that in UGe_2 the $5f$ electron itinerant description does not apply in the paramagnetic phase. The possibility that the character of the $5f$ electrons does not change across T_C should require alternative explanations of the effect of the magnetic interaction on the onset of superconductivity.

ACKNOWLEDGMENTS

This work was partly supported by a KBN Grant No. 2 PO3B 109 24. We thank Professor T. Komatsubara for his kind help in synthesis of single crystals and J. Stępień–Damm and D. Badurski for assistance with crystal preparation and indexing. Moreover, we wish to thank J. Rusz and A. Rubaszek for interesting and stimulating discussions and G. Ferro for help with instrumentation.

*Corresponding author. Also at Istituto Nazionale di Fisica della Materia, Corso Perrone 24, 16152 Genova, Italy. Email address: Biasini@bologna.enea.it

[1] P. Fulde and G. Zwicknagl, Physica B **206-207**, 125 (1995); G. Zwicknagl, Phys. Scr., T **T49**, 34 (1993), and references therein.

[2] S.S. Saxena, P. Agarwal, K. Ahilan, F.M. Grosche, R.K.W. Haselwimmer, M.J. Steiner, E. Pugh, I.R. Walker, S.R. Julian, P. Monthoux, G.G. Lonzarich, A. Huxley, I. Sheikin, D. Braithwaite, and J. Flouquet, Nature (London) **406**, 507 (2000), and references therein.

[3] See, for example, Y. Onuki and A. Hasegawa, *Handbook on Physics and Chemistry of Rare Earth* (Elsevier, 1995), Vol. 20, Chap. 135, and references therein.

[4] R. Settai, M. Nakashima, S. Araki, T.C. Kobayashi, N. Tateiwa, H. Yamagami, and Y. Onuki, J. Phys.: Condens. Matter **14**, L29 (2002).

[5] Y. Haga, M. Nakashima, R. Settai, S. Ikeda, T. Okubo, S. Araki, T.C. Kobayashi, N. Tateiwa, and Y. Onuki, J. Phys.: Condens. Matter **14**, L125 (2002).

[6] T. Terashima, T. Matsumoto, C. Terakura, S. Uji, N. Kimura, M. Endo, T. Komatsubara, and H. Aoki, Phys. Rev. Lett. **87**, 166401 (2001).

[7] C. Pfleiderer and A.D. Huxley, Phys. Rev. Lett. **89**, 147005 (2002), and references therein.

[8] R. Troc, Acta Phys. Pol. B **34**, 407 (2003), and references therein.

[9] A. Menovsky, F.R. de Boer, P.H. Frings, and J.J.M. Franse, in *High Field Magnetism*, edited by M. Date (North-Holland, Amsterdam, 1983), p. 189.

[10] S.K. Chan, J. Phys. Chem. Solids **32**, 1111 (1971).

[11] A.B. Shick and W.E. Pickett, Phys. Rev. Lett. **86**, 300 (2001).

[12] D.J. Singh and I.I. Mazin, Phys. Rev. Lett. **88**, 187004 (2002).

[13] Y. Onuki, S.W. Yun, I. Ukon, I. Umehara, K. Satoh, I. Sakamoto, M. Hunt, P. Meeson, P.A. Probst, and M. Springford, J. Phys. Soc. Jpn. **60**, 2127 (1991).

[14] S. Berko, in *Proceedings of the International School of Physics "Enrico Fermi,"* Course LXXXIII, edited by W. Brandt and A. Dupasquier (North-Holland, Amsterdam, 1983), p. 64.

[15] D.G. Lock, V.H. Crisp, and R.N. West, J. Phys. F: Met. Phys. **3**, 561 (1973).

[16] J.H. Kaiser, R.N. West, and N. Shiotani, J. Phys. F: Met. Phys. **16**, 1307 (1986).

[17] A. Rubaszek, Z. Szotek, and W.M. Temmermann, Phys. Rev. B **63**, 165115 (2001).

[18] P. Blaha, K. Schwartz, and J. Luitz, computer code WIEN97 (Tech. Universität Wien, Austria, 1999), ISBN 3-9501031-0-4.

[19] M. Biasini, G. Ferro, M. Monge, G. di Francia, and V. La Ferrara, J. Phys.: Condens. Matter **12**, 5961 (2000).

[20] M. Biasini, G. Ferro, G. Kontrym-Sznajd, and A. Czopnik, Phys. Rev. B **66**, 075126 (2002).

[21] H. Haghighi, J.H. Kaiser, S. Rayner, R.N. West, J.Z. Liu, R. Shelton, R.H. Howell, F. Solal, and M.J. Fluss, Phys. Rev. Lett. **67**, 382 (1991).

[22] G. Zwicknagl, A.N. Yaresko, and P. Fulde, Phys. Rev. B **65**, 081103(R) (2003).

[23] J. Rusz and M. Biasini (unpublished).

[24] A. Yaouanc, P. Dalmas de Réotier, P.C.M. Gubbens, C.T. Kaiser, A.A. Menowsky, M. Mihalik, and S.P. Cottrell, Phys. Rev. Lett. **89**, 147001 (2002).

[25] See, for example, P. Fulde, *Electron Correlations in Molecules and Solids* (Springer-Verlag, Berlin 1991); Y. Onuki, T. Goto, and T. Kasuya, Mat. Sci. Technol. **3**, 545 (1991); S. Doniach. Physica B & C **91**, 231 (1977).

[26] Some authors denote the critical temperature for the change of nature of the *f* electrons as *coherence* temperature (Ref. 1) but its definition was never fully clarified.

[27] Jan Rusz (private communication).

[28] P. Genoud, A.A. Manuel, E. Walker, and M. Peter, J. Phys.: Condens. Matter **3**, 4201 (1991).

[29] M. Biasini, G. Ferro, and A. Czopnik, Phys. Rev. B **68**, 094513 (2003).

[30] H.H. Hill, in *Plutonium 1970 and other Actinides*, edited by W.M. Miner (Met. Soc. AIME, New York, 1970), p. 2.